# Supporting Information

# Slow Magnetic Relaxation in 8-Coordinate Mn(II) Compounds

Li-Xin Wang [a,c†], Xiao-Fan Wu [b†], Xin-Xin Jin [b†], Jia-Yi Li [c], Bing-Wu Wang [b*], Ji-Yan Liu [a*], Jing Xiang [a,c*], Song Gao [b,d]

[a.] *Key Laboratory of Optoelectronic Chemical Materials and Devices (Ministry of Education), School of Optoelectronic Materials and Technology, Jianghan University, Wuhan, 430056 China.* xiangjing@yangtzeu.edu.cn.

[b.] *State Key Laboratory of Rare Earth Materials Chemistry and Applications and PKU-HKU Joint Laboratory on Rare Earth Materials and Bioinorganic Chemistry, Peking University, Beijing 100871, P. R. China. E-mail:* wangbw@pku.edu.cn

[c.] *College of Chemistry and Environmental Engineering, Yangtze University, Jingzhou 434020, Hubei, P. R. China.*

[d.] *School of Chemistry, Sun Yat-Sen University, Guangzhou, China.*

# Table of Supporting Information

**Physical measurement and instruments**

IR spectra were obtained from KBr discs using a Nicolet 360 FT-IR spectrophotometer. Electronic spectra were recorded using a PerkinElmer Lambda 19 spectrophotometer in 1 cm quartz cuvettes. ESI mass spectra were recorded using a PE-SCIEX API 150 EX single-quadruple mass spectrometer. Elemental analysis was carried out by using an Elementar Vario EL Analyzer. PXRD patterns were collected using an X-ray diffractometer (Empyream, PANalytical B.V.) with a Cu-$K_\alpha$ radiation source. The powder samples for magnetic analysis were made from their crystal samples. The magnetic properties, including the variable-temperature magnetic susceptibility, field dependence of magnetization, and ac magnetic susceptibility, were investigated using a Quantum Design MPMS XL-7 or VSM SQUID system. Background corrections were done experimentally on the corresponding sample holder. The diamagnetism of the constituent atoms (Pascal's tables) was used to correct the experimental susceptibilities.

**Crystal structures determination for 1-4.**

Crystal samples of **1–4** that are suitable for X-ray diffraction analysis were obtained by slow evaporation of their methanolic solutions. X-ray diffraction data for **1–4** were collected at low temperature (100 K) on an Oxford CCD diffractometer (Mo K\α, λ = 0.71073 Å). Their structures were resolved using Olex2 platform[1] by the Intrinsic Phasing method with SHELXT-2018 program[2] and refined by full-matrix least-squares using SHELXL-2018 [3] and expanded using Fourier techniques. CCDC number **2207891-2207894** contain supplementary crystallographic data for compounds **1–4**, which were deposited with the Cambridge Crystallographic Data Centre, CCDC, 12 Union Road, Cambridge CB21EZ, U.K.

**Computational Details.**

The *ab initio* calculations on the magnetic properties were done by MOLCAS 8.0, using the X-ray structure of the complexes with counterions omitted. The basis sets are ano-rcc-vtzp for Mn atoms, ano-rcc-vdzp for the coordinated N and O atoms, and ano-rcc-vdz for other atoms, using basis libraries from the MOLCAS package. For the complete active space self-consistent field (CASSCF) calculations, the active space consists of five electrons distributed in the five 3d orbitals of the Mn metal center. The doublet, quartet, and sextet were considered in the calculations. CASPT2 calculations were performed after CASSCF. The low-lying spin−orbit coupling states were then computed by RASSI-SO calculations. Finally, local magnetic properties (energy levels, D tensors, g-tensors, main magnetic axes, local magnetic susceptibility, etc.) of the complexes were calculated by the SINGLE_ANISO program. The lowest-energy vertical electronic transitions of the Mn(II) complexes were calculated by GAUSSIAN 09.[4] An M06 functional[5] and a mixed basis set of 6-31+G(d,p)[6] (for other elements) and LANL2DZ effective core potential[7] (for Mn atoms) were employed in the calculations. The solvent effect was taken into account by the polarized continuum model (PCM).[8] Frequency calculations were done on the optimized ground state structures, and no imaginary frequencies were found.

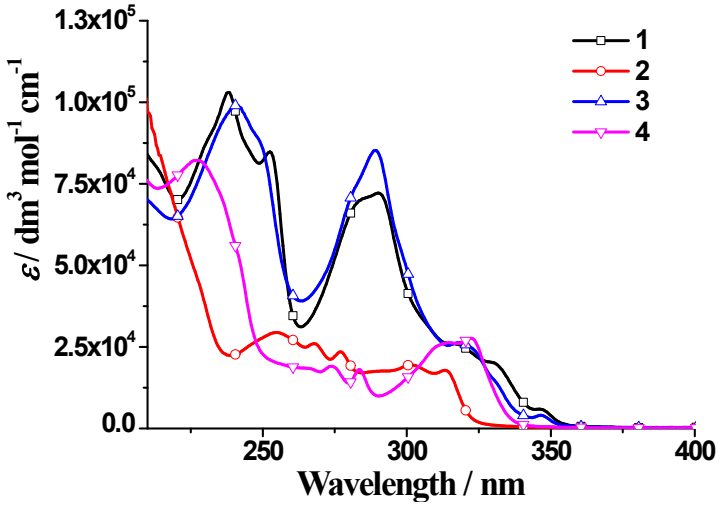


**Figure S1**. The UV/Vis spectra of compounds **1-4** in MeCN.

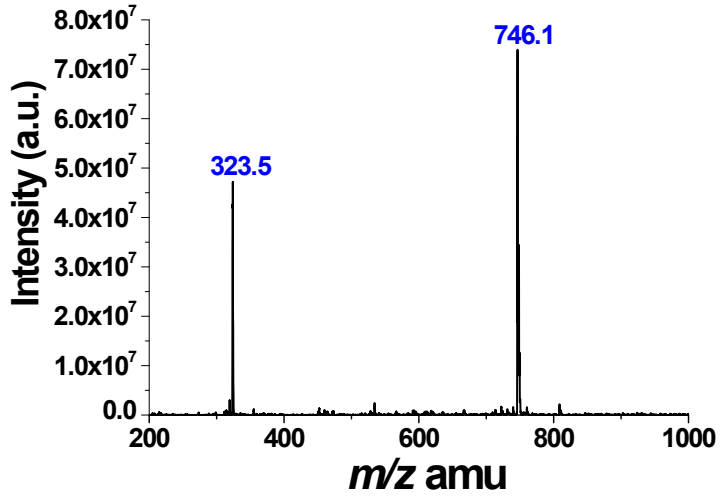


**Figure S2**. ESI/MS (+ve mode) of **1** in MeOH.

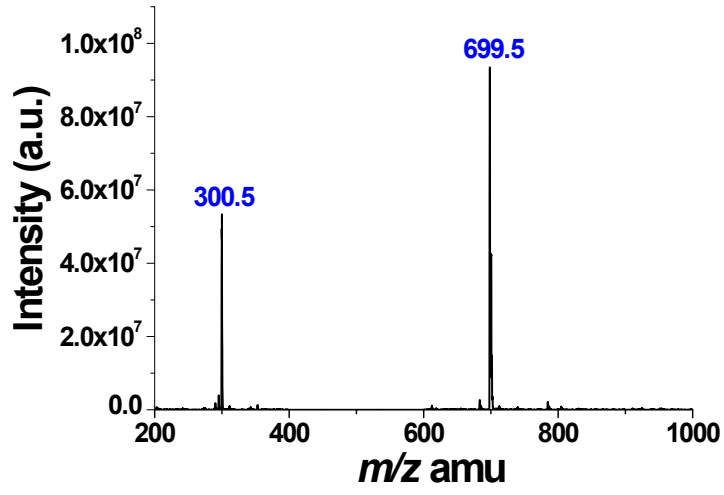


**Figure S3**. ESI/MS (+ve mode) of **2** in MeOH.

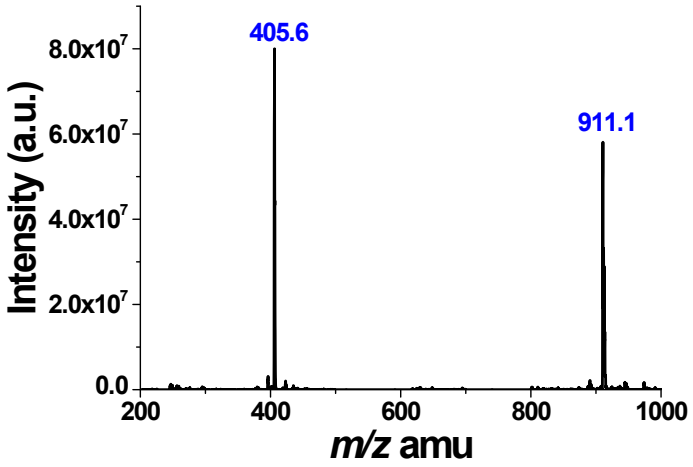


**Figure S4**. ESI/MS (+ve mode) of **3** in MeOH.

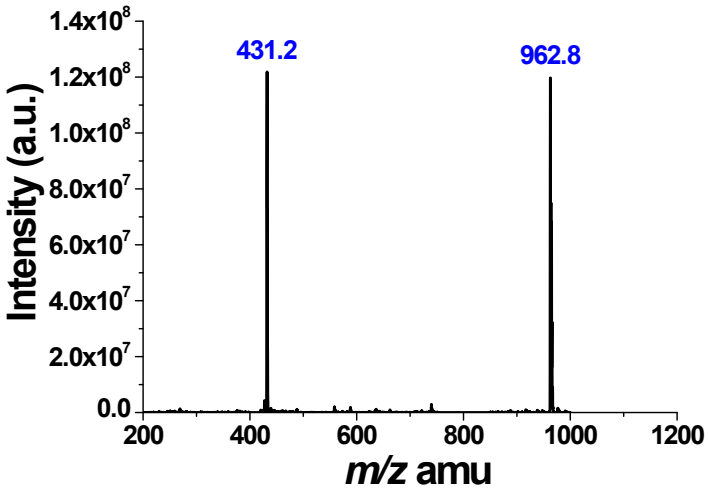


**Figure S5**. ESI/MS (+ve mode) of **4** in MeOH.

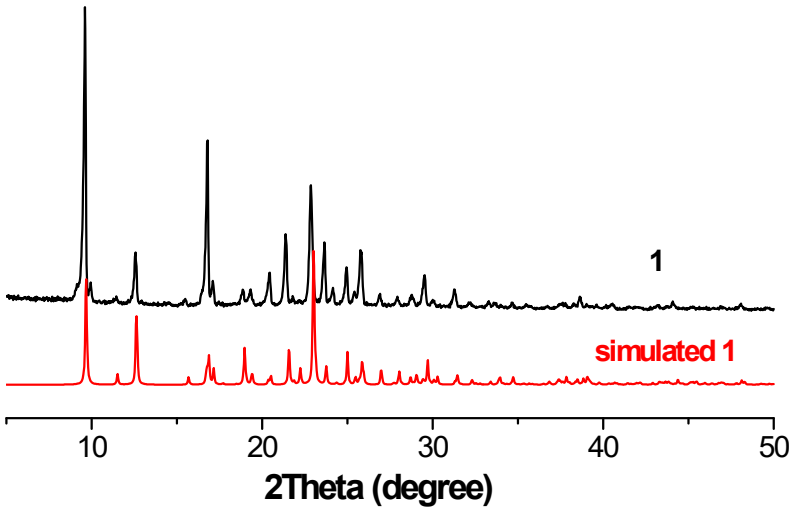


**Figure S6.** The simulated and synthesized PXRD patterns of compound **1.**

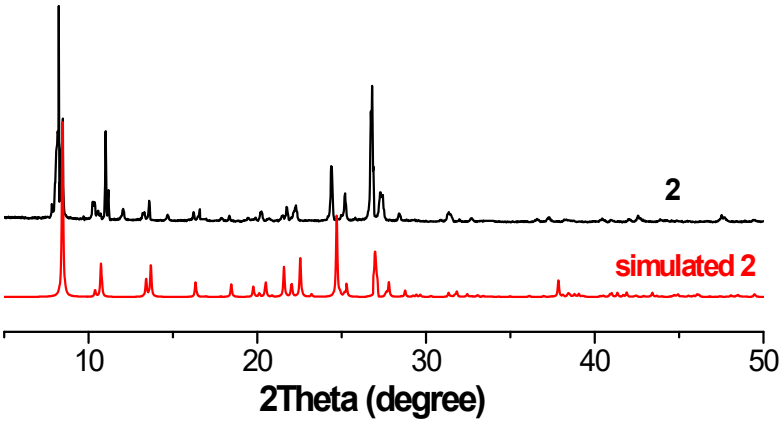


**Figure S7.** The simulated and synthesized PXRD patterns of compound **2**.

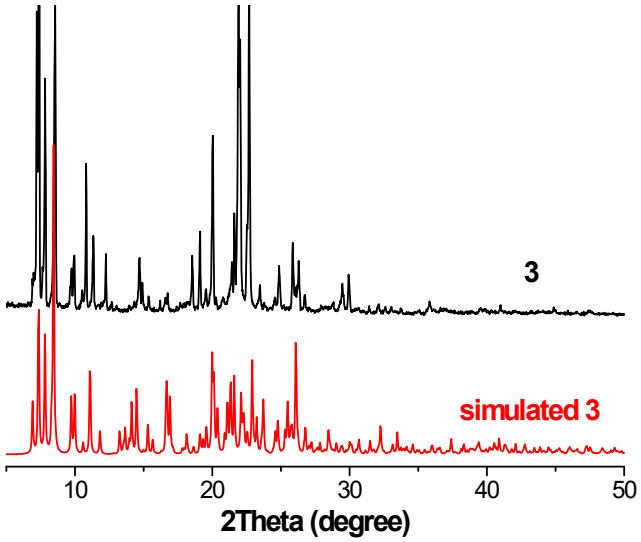


**Figure S8.** The simulated and synthesized PXRD patterns of compound **3.**

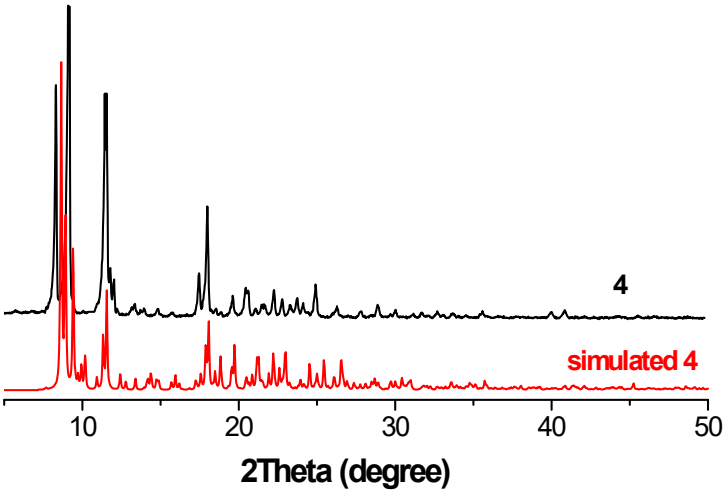


**Figure S9.** The simulated and synthesized PXRD patterns of compound **4.**

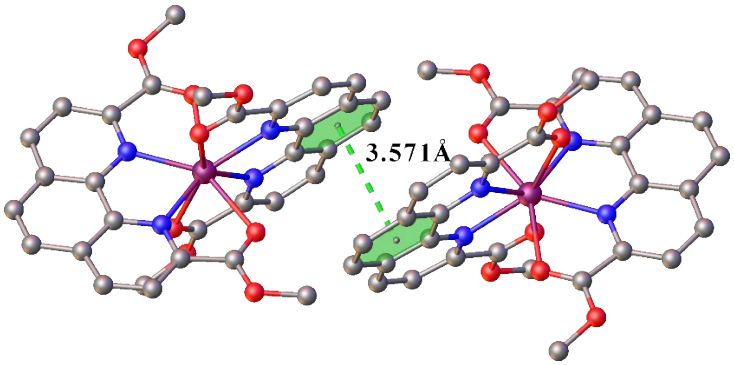


**Figure S10**. The intermolecular π···π stacking interaction in compound **1**.

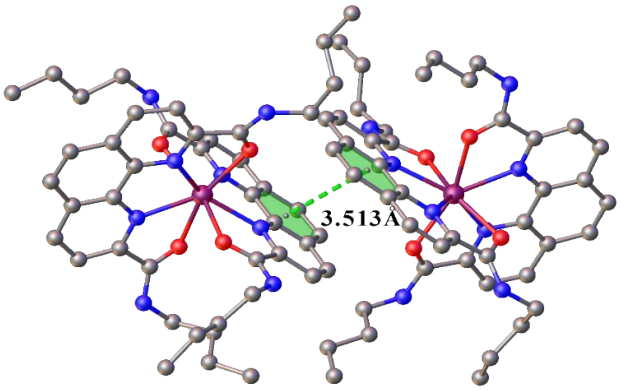


**Figure S11**. The intermolecular π···π stacking interaction in compound **3**.

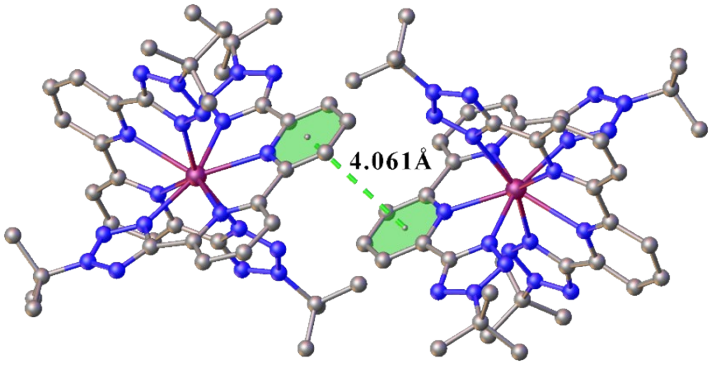


**Figure S12**. The intermolecular π···π stacking interaction in compound **4**.

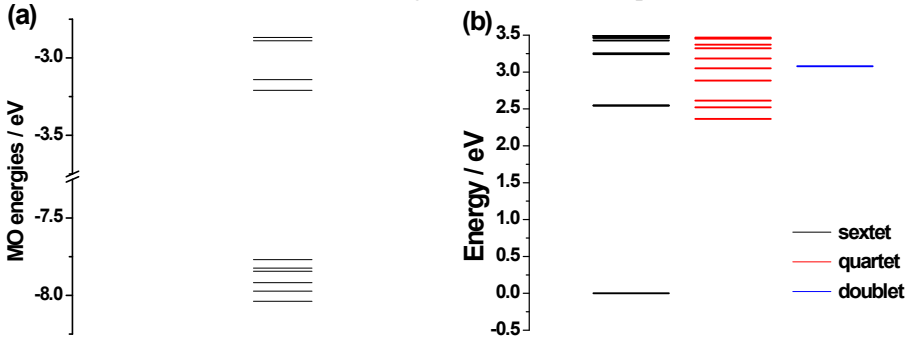


**Figure S13** (a) The MO energy levels of the sextet for **3**; (b) The energy level of three spin states for **3**.

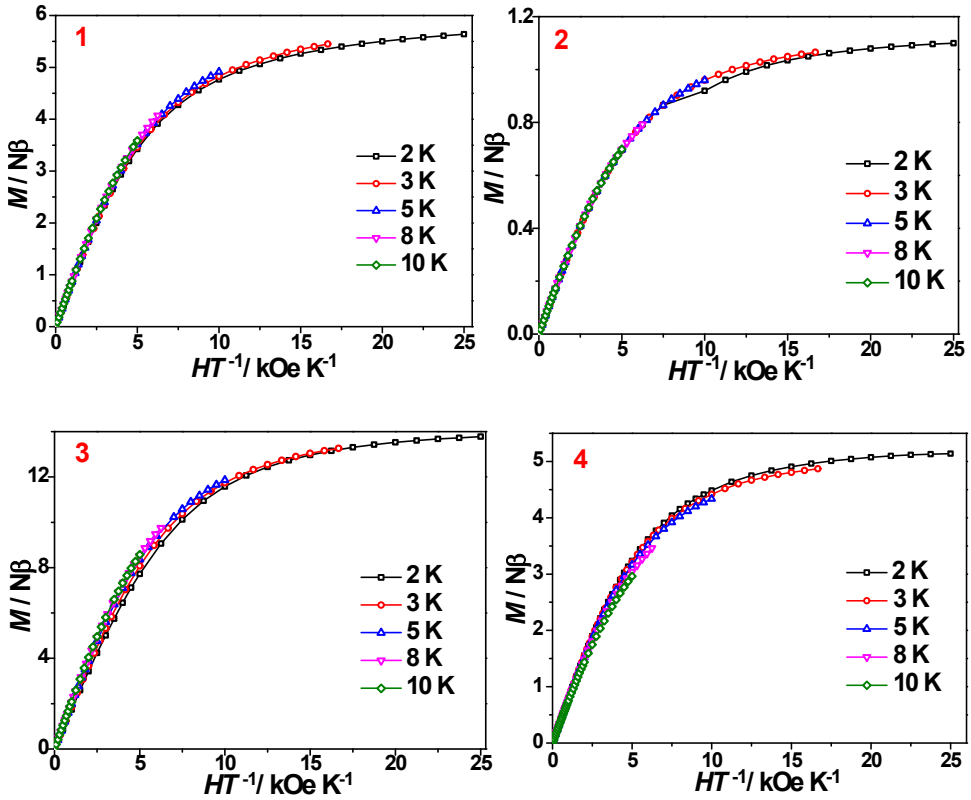


**Figure S14**. The magnetization data for **1-4** collected under various dc fields *M vs.* $HT^{-1}$ plots.

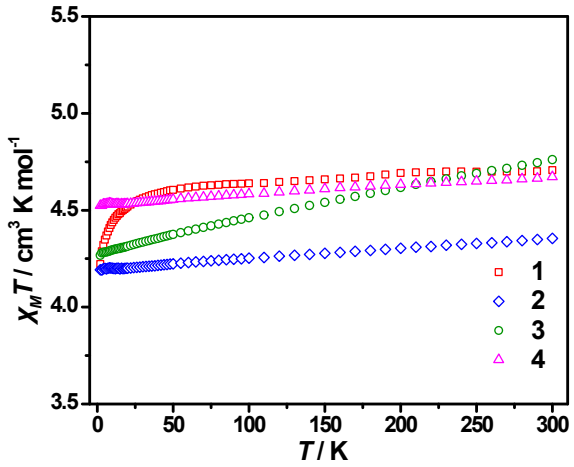


**Figure S15.** Temperature dependence of $\chi_M T$ *vs.* *T* for **1-4** measured at 1 kOe.

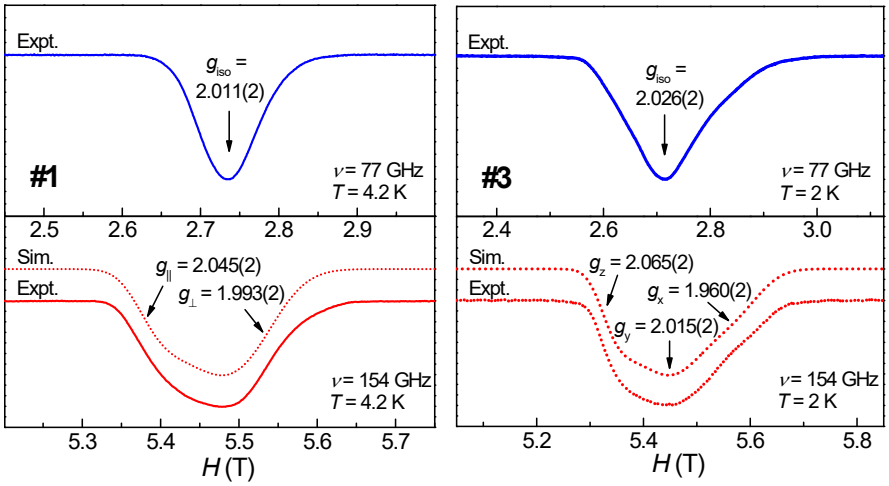


**Figure S16**. The multifrequency fine-structure high field-EPR spectroscopy of compounds **1** and **3.**

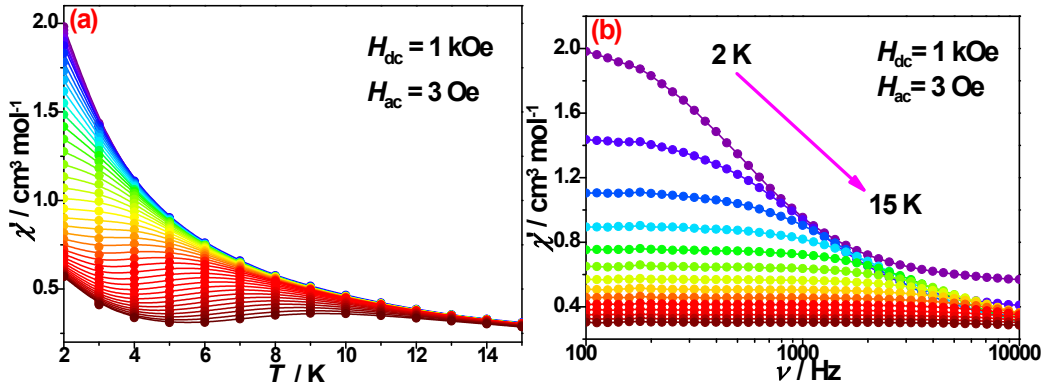


**Figure S17**. (a) Temperature dependence of the in-phase ($\chi'$) signal of the *ac* magnetic susceptibility for **1** ($H_{dc}$ = 1 kOe and $H_{ac}$ = 3 Oe); (b) Frequency dependence of in-phase ($\chi'$) *ac* magnetic susceptibility for **1**.

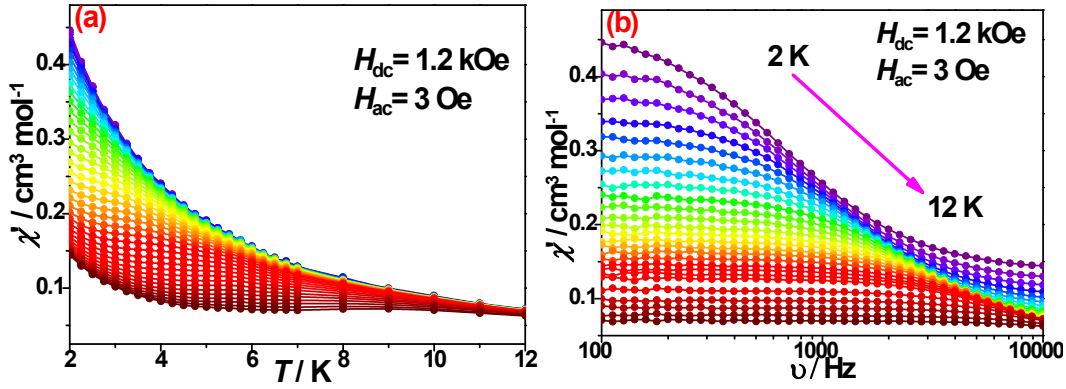


**Figure S18**. (a) Temperature dependence of the in-phase ($\chi'$) signal of the *ac* magnetic susceptibility for **2** ($H_{dc}$ = 1.2 kOe and $H_{ac}$ = 3 Oe); (b) Frequency dependence of in-phase ($\chi'$) *ac* magnetic susceptibility for **2**.

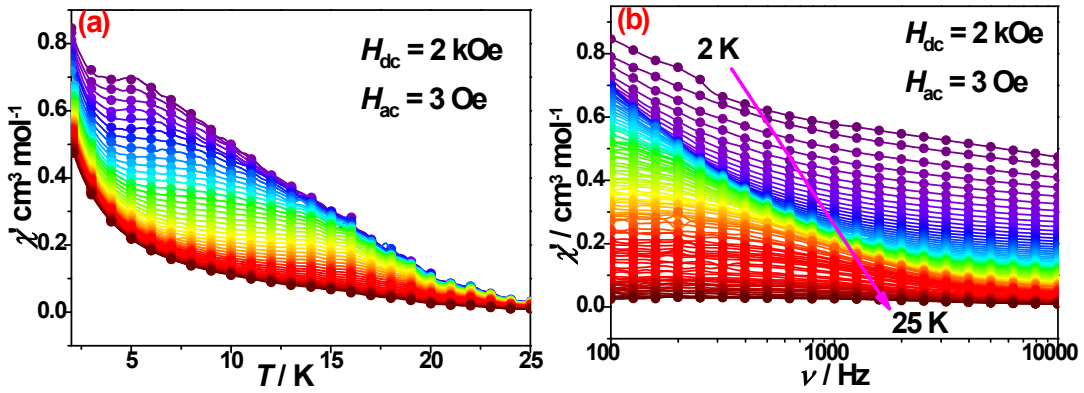


**Figure S19**. (a) Temperature dependence of the in-phase ($\chi'$) signal of the *ac* magnetic susceptibility for **3** ($H_{dc}$ = 2 kOe and $H_{ac}$ = 3 Oe); (b) Frequency dependence of in-phase ($\chi'$) *ac* magnetic susceptibility for **3**.

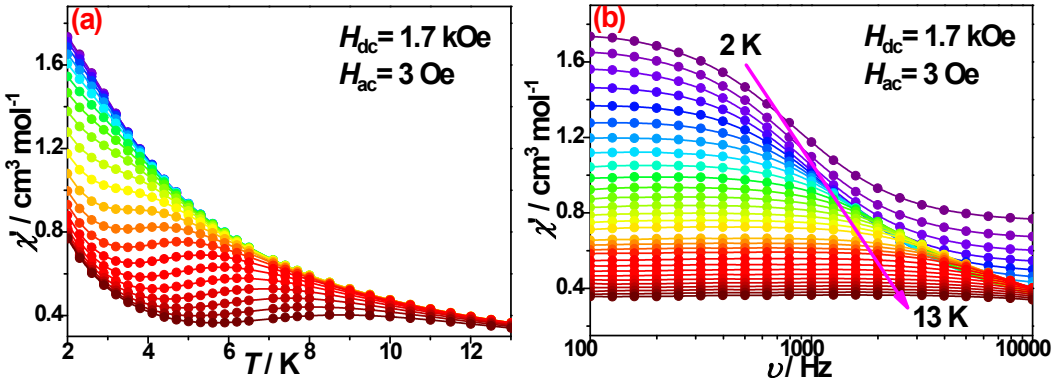


**Figure S20**. (a) Temperature dependence of the in-phase ($\chi'$) signal of the *ac* magnetic susceptibility for **4** ($H_{dc}$ = 1.7 kOe and $H_{ac}$ = 3 Oe); (b) Frequency dependence of in-phase ($\chi'$) *ac* magnetic susceptibility for **4**.

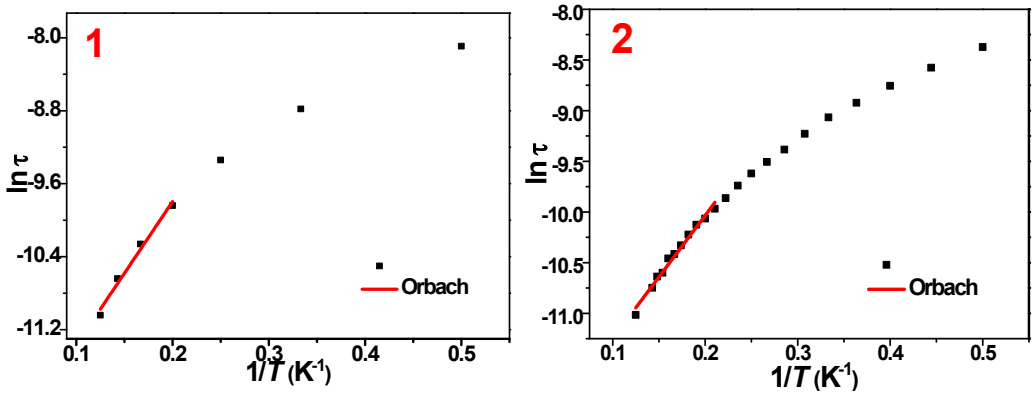

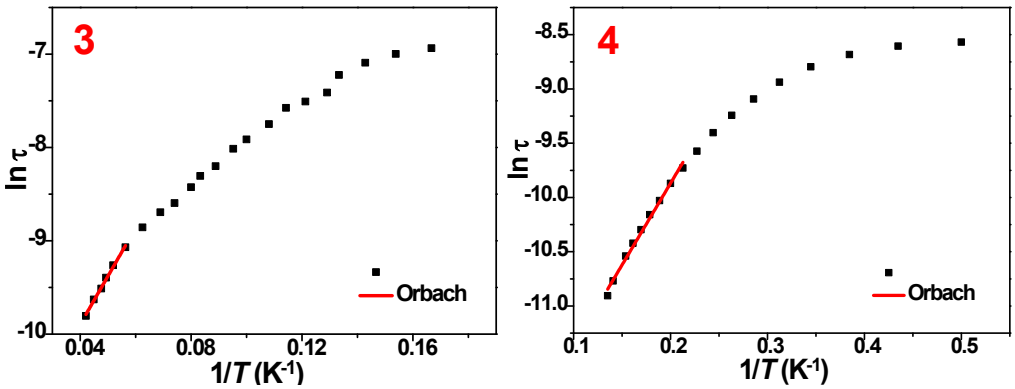


**Figure S21**. The ln(τ) *vs*. 1/*T* plots for **1, 2**, ,**3,** and **4**, the red line represents the fit of Orbach process.

**Table S1**. The calculated Continuous Shape Measures (CShM) for **1.**

| Square antiprism ($D_{4d}$) | Triangular dodecahedron (***D*****$_{2d}$**) | Biaugmented trigonal prism J50 ($C_{2v}$) | Biaugmented trigonal prism ($C_{2v}$) | Snub diphenoid J84 ($D_{2d}$) | Cube (Oh) |
|---|---|---|---|---|---|
| 3.973 | **1.378** | 4.094 | 2.653 | 5.235 | 12.150 |

**Table S2**. The calculated Continuous Shape Measures (CShM) for **2.**

| Square antiprism ($D_{4d}$) | Triangular dodecahedron (***D*****$_{2d}$**) | Cube (Oh) | Biaugmented trigonal prism J50 ($C_{2v}$) | Biaugmented trigonal prism ($C_{2v}$) | Snub diphenoid J84 ($D_{2d}$) |
|---|---|---|---|---|---|
| 2.503 | **1.070** | 12.458 | 3.752 | 2.551 | 4.235 |

**Table S3**. The calculated Continuous Shape Measures (CShM) for **3.**

| Square antiprism ($D_{4d}$) | Triangular dodecahedron (***D*****$_{2d}$**) | Biaugmented trigonal prism J50 ($C_{2v}$) | Biaugmented trigonal prism ($C_{2v}$) | Johnson gyrobifastigium J26 ($D_{2d}$) | Snub diphenoid J84 ($D_{2d}$) |
|---|---|---|---|---|---|
| 4.009 | **1.703** | 3.491 | 2.578 | 11.639 | 3.820 |

**Table S4**. The calculated Continuous Shape Measures (CShM) for **4.**

| Square antiprism ($D_{4d}$) | Triangular dodecahedron (***D*****$_{2d}$**) | Johnson gyrobifastigium J26 ($D_{2d}$) | Biaugmented trigonal prism J50 ($C_{2v}$) | Biaugmented trigonal prism ($C_{2v}$) | Snub diphenoid J84 ($D_{2d}$) |
|---|---|---|---|---|---|
| 4.094 | **1.645** | 10.820 | 3.380 | 2.794 | 2.711 |

**Table S5**. Crystal data and structure refinement details for compounds **1-4.**

| | **1** | **2** | **3** | **4** |
|---|---|---|---|---|
| Formula | $C_{32}H_{24}Cl_2MnN_4O_{16}$•2 | $C_{28}H_{24}Cl_2MnN_4$ | $C_{44}H_{52}Cl_2MnN_8O_{12}$• | $C_{40}H_{48}Cl_2MnN_{20}O_8$ |

| | $CH_3OH$ | $O_{16}$ | $H_2O$ | |
|---|---|---|---|---|
| *Mr* | 910.47 | 798.35 | 1028.79 | 1062.82 |
| *T* /K | 100.0 (1) | 100.0 (2) | 100.0 (1) | 100.0 (1) |
| Crystal syst. | Monoclinic | Orthorhombic | Monoclinic | Monoclinic |
| Space group | *C*2/*c* | *Pban* | $P2_1/n$ | $P2_1/c$ |
| *a*/Å | 22.5798 (16) | 9.9383 (13) | 13.8971 (2) | 10.937 (2) |
| *b*/Å | 10.5896 (6) | 16.4516 (16) | 21.2744 (3) | 39.707 (8) |
| *c*/Å | 18.9921 (10) | 10.4468 (10) | 16.6480 (3) | 12.853 (3) |
| *α*, (°) | 90 | 90 | 90 | 90 |
| *β*, (°) | 126.041 (7) | 90 | 106.152 (2) | 110.80 (3) |
| *γ*, (°) | 90 | 90 | 90 | 90 |
| *V*/ Å$^3$ | 3672.0 (5) | 1708.5 (3) | 4727.74 (14) | 5218 (2) |
| *Z* | 4 | 2 | 4 | 4 |
| $\rho_{calcd}$, Mg m$^{-3}$ | 1.647 | 1.552 | 1.445 | 1.353 |
| F(000) | 1868 | 814 | 2148 | 2204 |
| Collected refl. | 9213 | 5694 | 19999 | 25913 |
| Unique refl. | 3819 | 1780 | 9288 | 9174 |
| *R*(int) | 0.036 | 0.054 | 0.031 | 0.075 |
| Final *R* indices | $R_1$(obs)=0.06 | 0.064 | $R_1$(obs)=0.037 | 0.098 |
| $I > 2\sigma(I)$ | *w*R(all)=0.146 | *w*R(all)=0.180 | *w*R(all)=0.099 | *w*R(all)=0.196 |
| GOF | 1.10 | 1.11 | 1.04 | 1.18 |
| No. of par. | 271 | 185 | 625 | 652 |

**Table S6.** Calculated lowest 10 electronic transitions of the sextet ($S$ = 5/2) state for **3**.

| Excited state | $\lambda_{calc}$/nm (Oscillator Strength) | Changes of the electron density (% contribution; H: HOMO, L: LUMO) | Transition Character |
|---|---|---|---|
| 1 | 487.2 (0) | Alpha:<br>H-6→L+2 (1.3), H-4→L (4.6), H-4→L+1 (5.9), **H-2→L (11.3)**, **H-2→L+1 (8.4)**, H-1→L (1.7), H-1→L+1 (5.1), H→L+1 (1.1)<br>Beta:<br>H-2→L+2 (1.2), **H-1→L (12.0)**, **H-1→L+1** | LC+MLCT |

| | | | |
|---|---|---|---|
| | | **(17.3)**, H→L (7.5), H→L+1 (2.9) | |
| 2 | 486.9 (0) | Alpha:<br>H-7→L+4 (1.0), H-5→L (1.7), H-5→L+1 (1.5), H-3→L (4.3), H-3→L+1 (3.1), H-2→L (3.8), **H-2→L+1 (6.7)**, **H-1→L (11.5)**, **H-1→L+1 (6.5)**<br>Beta:<br>H-2→L+3 (1.1), H-1→L (7.9), H-1→L+1 (2.2), **H→L (14.1)**, **H→L+1 (15.8)** | LC+MLCT |
| 3 | 382.3 (0.0001) | Alpha:<br>H-4→L+2 (7.7), **H-2→L+2 (18.4)**, H-1→L+2 (7.3), H→L+2 (2.4)<br>Beta:<br>**H-1→L+2 (29.2)**, H→L+2 (9.7) | LC+MLCT |
| 4 | 381.0 (0.0001) | Alpha:<br>H-7→L (1.2), H-5→L+3 (2.1), H-3→L+3 (5.6), H-2→L+3 (9.2), **H-1→L+3 (17.9)**<br>Beta:<br>H-3→L (1.2), H-1→L+3 (9.0), **H→L+3 (29.3)** | LC+MLCT |
| 5 | 361.8 (0.0005) | Alpha:<br>**H-4→L (27.6)**, **H-4→L+1 (14.7)**, H-4→L+3 (3.0), H-3→L+3 (2.5), H-2→L (6.3), H-2→L+1 (5.2), H-1→L (9.2), H-1→L+1 (3.1), H-1→L+3 (2.8), H→L (9.7), H→L+1 (2.4) | LC+MLCT |
| 6 | 358.0 (0.0001) | Alpha:<br>H-5→L+1 (1.8), H-5→L+2 (3.1), H-4→L (3.0), H-4→L+1 (3.9), **H-4→L+3 (13.5)**, **H-3→L (19.9)**, H-3→L+2 (3.3), H-2→L (6.9), H-2→L+2 (1.6), H-2→L+3 (5.1), H-1→L+1 (3.5), H-1→L+2 (2.1), H-1→L+3 (1.4), **H→L (13.8)** | LC+MLCT |
| 7 | 357.3 (0.0005) | Alpha:<br>**H-5→L (14.0)**, **H-5→L+1 (9.1)**, H-4→L (1.2), H-4→L+3 (3.9), H-3→L (1.3), **H-3→L+1 (12.2)**, H-3→L+2 (5.0), H-2→L+1 (3.9), H-2→L+3 (1.9), **H-1→L (11.2)**, **H-** | LC+MLCT |

| | | | |
|---|---|---|---|
| | | **1→L+1 (9.0)**, H-1→L+2 (2.2), H→L (7.6), H→L+2 (2.6) | |
| 8 | 355.8 (0) | Alpha:<br>H-7→L (3.7), H-7→L+1 (3.6), H-7→L+2 (5.0), **H-6→L (5.1)**, H-6→L+1 (3.9), **H-6→L+2 (5.0)**, H-6→L+3 (1.1), H-5→L+2 (2.7), H-4→L+3 (3.6), H-3→L+1 (2.4), H-2→L+5 (1.0), H-1→L+2 (2.7), H→L (2.9), H→L+1 (1.9)<br>Beta:<br>**H-3→L (5.2)**, H-3→L+1 (4.0), **H-3→L+2 (6.1)**, **H-2→L (5.6)**, H-2→L+1 (3.1), **H-2→L+2 (5.1)**, H-2→L+3 (1.6), H-1→L+2 (1.6), H-1→L+5 (1.3) | LC+MLCT |
| 9 | 355.0 (0.0003) | Alpha:<br>H-7→L (2.8), **H-7→L+1 (5.6)**, H-7→L+3 (3.0), **H-6→L (6.7)**, H-6→L+1 (1.0), H-6→L+2 (1.1), H-6→L+3 (1.5), H-5→L (1.1), H-5→L+2 (2.7), H-4→L+3 (3.0), H-3→L+1 (1.1), H-3→L+3 (2.2), H-1→L+1 (1.3), H-1→L+2 (1.7), H-1→L+3 (2.3), **H→L (15.1)**<br>Beta:<br>H-3→L (2.4), H-3→L+1 (4.6), H-3→L+3 (3.4), **H-2→L (8.5)**, H-2→L+1 (1.3), H-2→L+3 (2.3), H→L+3 (1.8), H→L+4 (1.1) | LC+MLCT |
| 10 | 354.8 (0.0004) | Alpha:<br>H-7→L (6.1), H-7→L+1 (3.0), H-7→L+2 (1.3), H-6→L (2.9), H-6→L+1 (4.0), H-6→L+2 (2.5), H-5→L (1.4), H-5→L+1 (1.5), **H-5→L+2 (5.7)**, H-4→L+3 (2.7), H-2→L (2.2), H-2→L+3 (3.4), H-1→L (3.8), H-1→L+2 (2.1), H-1→L+4 (1.1), **H→L (13.0)**, H→L+1 (1.3)<br>Beta:<br>**H-3→L (6.3)**, H-3→L+1 (2.9), H-3→L+2 (1.4), H-2→L (3.6), H-2→L+1 (4.0), H-2→L+2 (2.6), H→L+3 (2.2), H→L+4 (1.5) | LC+MLCT |

**Table S7.** Calculated lowest 10 electronic transitions of the quartet (S = 3/2) state for **3**.

| Excited state | $\lambda_{calc}$/nm (Oscillator Strength) | Changes of the electron density (% contribution; H:HOMO, L:LUMO) | Transition Character |
|---|---|---|---|
| 1 | 7927.0 (0) | Alpha:<br>H→L+1 (1.9), H→L+2 (1.2)<br>Beta:<br>H→L+10 (5.1), H→L+11 (12.8), H→L+13 (8.2), H→L+16 (2.2), **H→L+17 (57.1)**, H→L+18 (4.6), H→L+19 (2.1), H→L+28 (0.4) | d-d+LC |
| 2 | 5009.2 (0.0001) | Alpha:<br>H-4→L+1 (1.0)<br>Beta:<br>H→L+2 (15.2), H→L+5 (1.1), H→L+11 (1.7), H→L+12 (3.4), H→L+13 (4.2), **H→L+14 (22.2)**, **H→L+15 (34.4)**, H→L+16 (13.1) | d-d+LC |
| 3 | 2393.1 (0) | Alpha:<br>H-12→L+1 (1.4), H-11→L+1 (3.6), H-11→L+2 (2.3), H-2→L+1 (1.8), H-2→L+2 (1.1), H-1→L+1 (2.6), H-1→L+2 (1.6), **H→L+1 (47.0)**, **H→L+2 (29.6)**, H→L+3 (1.2),<br>Beta:<br>H→L+11 (0.4), H→L+13 (1.0), H→L+17 (1.0), H→L+28 (1.6) | d-d+LC |
| 4 | 1806.6 (0.0006) | Alpha:<br>H-28→L+1 (1.3), H-27→L+1 (3.1), H-27→L+2 (2.0), H-5→L+1 (10.4), H-5→L+2 (6.5), **H-3→L+1 (18.5)**, **H-3→L+2 (11.7)**, H-2→L+1 (1.2)<br>Beta:<br>H→L+3 (6.8), H→L+23 (3.8), **H→L+27 (14.0)**, H→L+28 (3.6) | d-d+LC |
| 5 | 1516.0 (0.0008) | Alpha:<br>H-37→L+1 (1.0), H-35→L+1 (1.6), H-35→L+2 (1.0), H-2→L+1 (8.4), H-2→L+2 (5.4), **H-1→L+1 (31.5)**, **H-1→L+2 (19.9)**, H→L+1 (3.5), H→L+2 (1.6), | d-d+MLCT |

| | | | |
|---|---|---|---|
| | | Beta:<br>**H→L+1 (17.2)** | |
| 6 | 1296.2<br>(0.0028) | Alpha:<br>H-27→L+1 (1.2), H-5→L+1 (4.9), H-5→L+2 (3.0), H-3→L+1 (9.2), H-3→L+2 (6.3), H-2→L+1 (4.9), H-2→L+2 (3.3)<br>Beta:<br>H→L (6.2), H→L+1 (1.7), **H→L+3 (21.6)**, H→L+22 (1.2), H→L+23 (5.2), **H→L+27 (16.6)**, H→L+28 (4.0) | d-d+MLCT |
| 7 | 1234.0<br>(0.0002) | Alpha:<br>H-31→L+1 (4.7), H-31→L+2 (3.0), **H-4→L+1 (27.8)**, **H-4→L+2 (17.5)**, H-2→L+1 (9.9), H-2→L+2 (6.2), H-1→L+1 (6.4), H-1→L+2 (3.9)<br>Beta:<br>H→L+1 (3.4), H→L+2 (6.4), H→L+3 (1.3), H→L+14 (0.2), H→L+15 (0.3), | d-d+LC |
| 8 | 1139.4<br>(0.037) | Alpha:<br>H-2→L+1 (2.8), H-2→L+2 (1.5), H-1→L+1 (3.0), H-1→L+2 (1.7)<br>Beta:<br>**H→L (52.2)**, **H→L+1 (34.1)** | MLCT+d-d |
| 9 | 1125.5<br>(0.0087) | Alpha:<br>H-2→L+1 (1.9), H-1→L+1 (2.1), H-1→L+2 (1.3)<br>Beta:<br>**H→L (38.9)**, **H→L+1 (38.1)**, H→L+3 (6.7), H→L+27 (4.1) | MLCT+d-d |
| 10 | 1025.2<br>(0.0007) | Beta:<br>H→L+2 (2.4), H→L+3 (1.4), H→L+16 (1.9), H→L+17 (1.6), H→L+19 (1.4), H→L+22 (1.3), H→L+23 (3.3), H→L+25 (3.7), H→L+26 (3.2), H→L+27 (17.3), **H→L+28 (47.7)**, H→L+29 (1.8), H→L+31 (2.6), H→L+32 (3.1) | MLCT+d-d |

**Table S8.** Parameters of one-component Debye's model for compound **1**.

| $T$ / K | $\chi_S$ / (cm$^3$ mol$^{-1}$) | $\chi_T$ / (cm$^3$ mol$^{-1}$) | $\tau$ / (s) | $\alpha$ | ***Residual*** |
|---|---|---|---|---|---|
| 2.0 | 0.555769E+00 | 0.209034E+01 | 0.304723E-03 | 0.832914E-01 | 0.995429E-03 |
| 3.0 | 0.385112E+00 | 0.146188E+01 | 0.152988E-03 | 0.616705E-01 | 0.626242E-03 |
| 4.0 | 0.296002E+00 | 0.111625E+01 | 0.872608E-04 | 0.481572E-01 | 0.295111E-03 |
| 5.0 | 0.242327E+00 | 0.900461E+00 | 0.537851E-04 | 0.379323E-01 | 0.248168E-03 |
| 6.0 | 0.207240E+00 | 0.755892E+00 | 0.351255E-04 | 0.296442E-01 | 0.146490E-03 |
| 7.0 | 0.182811E+00 | 0.650665E+00 | 0.241288E-04 | 0.222930E-01 | 0.188391E-03 |

**Table S9.** Parameters of one-component Debye's model for compound **2**.

| $T$ / K | $\chi_S$ / (cm$^3$ mol$^{-1}$) | $\chi_T$ / (cm$^3$ mol$^{-1}$) | $\tau$ / (s) | $\alpha$ | ***Residual*** |
|---|---|---|---|---|---|
| 2.00 | 0.136743E+00 | 0.465280E+00 | 0.233306E-03 | 0.117371E+00 | 0.762541E-04 |
| 2.25 | 0.121972E+00 | 0.418521E+00 | 0.192101E-03 | 0.105934E+00 | 0.106774E-03 |
| 2.50 | 0.110386E+00 | 0.380142E+00 | 0.159849E-03 | 0.942033E-01 | 0.654830E-04 |
| 2.75 | 0.100605E+00 | 0.346803E+00 | 0.134565E-03 | 0.840014E-01 | 0.609857E-04 |
| 3.00 | 0.923677E-01 | 0.320747E+00 | 0.115341E-03 | 0.788883E-01 | 0.457252E-04 |
| 3.25 | 0.854417E-01 | 0.295943E+00 | 0.993156E-04 | 0.701006E-01 | 0.615971E-04 |
| 3.50 | 0.789879E-01 | 0.274443E+00 | 0.865259E-04 | 0.667030E-01 | 0.535294E-04 |
| 3.75 | 0.744930E-01 | 0.255070E+00 | 0.757206E-04 | 0.545716E-01 | 0.525430E-04 |
| 4.00 | 0.689021E-01 | 0.238557E+00 | 0.669286E-04 | 0.577528E-01 | 0.439142E-04 |
| 4.25 | 0.648533E-01 | 0.223947E+00 | 0.597755E-04 | 0.556014E-01 | 0.581250E-04 |
| 4.50 | 0.611957E-01 | 0.210222E+00 | 0.536534E-04 | 0.523177E-01 | 0.330877E-04 |
| 4.75 | 0.574047E-01 | 0.198384E+00 | 0.479414E-04 | 0.534139E-01 | 0.500615E-04 |
| 5.00 | 0.547383E-01 | 0.188637E+00 | 0.436118E-04 | 0.538520E-01 | 0.518267E-04 |
| 5.25 | 0.525864E-01 | 0.178814E+00 | 0.396266E-04 | 0.467224E-01 | 0.371055E-04 |
| 5.50 | 0.490967E-01 | 0.170464E+00 | 0.357550E-04 | 0.547421E-01 | 0.739508E-04 |
| 5.75 | 0.484285E-01 | 0.162681E+00 | 0.333572E-04 | 0.463518E-01 | 0.560218E-04 |
| 6.00 | 0.463494E-01 | 0.154315E+00 | 0.309853E-04 | 0.450804E-01 | 0.538901E-04 |
| 6.25 | 0.427641E-01 | 0.145794E+00 | 0.277720E-04 | 0.522690E-01 | 0.355199E-04 |

**Table S10.** Parameters of one-component Debye's model fo compound **3**.

| $T$ / K | $\chi_S$ / (cm$^3$ mol$^{-1}$) | $\chi_T$ / (cm$^3$ mol$^{-1}$) | $\tau$ / (s) | $\alpha$ | ***Residual*** |
|---|---|---|---|---|---|
| 6.0 | 0.172118E+00 | 0.101105E+01 | 0.112334E-02 | 0.241268E+00 | 0.567260E-03 |
| 6.5 | 0.158000E+00 | 0.923647E+00 | 0.927868E-03 | 0.233587E+00 | 0.650204E-03 |
| 7.0 | 0.144649E+00 | 0.865149E+00 | 0.810729E-03 | 0.235488E+00 | 0.281967E-03 |
| 7.5 | 0.135524E+00 | 0.786935E+00 | 0.667882E-03 | 0.219263E+00 | 0.309094E-03 |
| 8.0 | 0.125745E+00 | 0.736822E+00 | 0.589352E-03 | 0.217544E+00 | 0.161513E-03 |
| 8.5 | 0.118164E+00 | 0.690514E+00 | 0.519100E-03 | 0.210214E+00 | 0.220058E-03 |
| 9.0 | 0.110494E+00 | 0.648580E+00 | 0.466946E-03 | 0.207050E+00 | 0.207647E-03 |
| 9.5 | 0.103990E+00 | 0.608478E+00 | 0.416573E-03 | 0.199272E+00 | 0.171004E-03 |
| 10.0 | 0.987619E-01 | 0.569851E+00 | 0.372390E-03 | 0.188164E+00 | 0.470290E-03 |
| 10.5 | 0.930407E-01 | 0.534998E+00 | 0.332195E-03 | 0.180859E+00 | 0.250953E-03 |
| 11.0 | 0.873545E-01 | 0.506872E+00 | 0.307878E-03 | 0.177458E+00 | 0.622991E-03 |

| | | | | | |
|---|---|---|---|---|---|
| 11.5 | 0.827958E-01 | 0.470236E+00 | 0.270848E-03 | 0.162680E+00 | 0.263425E-03 |
| 12.0 | 0.789289E-01 | 0.438257E+00 | 0.243916E-03 | 0.148922E+00 | 0.388467E-03 |
| 12.5 | 0.751200E-01 | 0.418426E+00 | 0.224057E-03 | 0.144827E+00 | 0.252875E-03 |
| 13.0 | 0.703880E-01 | 0.388791E+00 | 0.204421E-03 | 0.137204E+00 | 0.531681E-03 |
| 13.5 | 0.683797E-01 | 0.373735E+00 | 0.186524E-03 | 0.125969E+00 | 0.430959E-03 |
| 14.0 | 0.647953E-01 | 0.351063E+00 | 0.170704E-03 | 0.119633E+00 | 0.215720E-03 |
| 14.5 | 0.612961E-01 | 0.333279E+00 | 0.159386E-03 | 0.115116E+00 | 0.223365E-03 |
| 15.0 | 0.573052E-01 | 0.309164E+00 | 0.147125E-03 | 0.111411E+00 | 0.300534E-03 |
| 15.5 | 0.530382E-01 | 0.294451E+00 | 0.135947E-03 | 0.118355E+00 | 0.345095E-02 |
| 16.0 | 0.520649E-01 | 0.273702E+00 | 0.129902E-03 | 0.913188E-01 | 0.127129E-02 |
| 16.5 | 0.454430E-01 | 0.241520E+00 | 0.118636E-03 | 0.993899E-01 | 0.858161E-03 |
| 17.0 | 0.413135E-01 | 0.217585E+00 | 0.114399E-03 | 0.100506E+00 | 0.173529E-03 |
| 17.5 | 0.381704E-01 | 0.198257E+00 | 0.110060E-03 | 0.907595E-01 | 0.256720E-03 |
| 18.0 | 0.356713E-01 | 0.178909E+00 | 0.103543E-03 | 0.795587E-01 | 0.491322E-03 |
| 18.5 | 0.327140E-01 | 0.166937E+00 | 0.963234E-04 | 0.849101E-01 | 0.301539E-03 |
| 19.0 | 0.292997E-01 | 0.145903E+00 | 0.915770E-04 | 0.778550E-01 | 0.146278E-02 |
| 19.5 | 0.236278E-01 | 0.125594E+00 | 0.935635E-04 | 0.113999E+00 | 0.736773E-03 |
| 20.0 | 0.202954E-01 | 0.108921E+00 | 0.937819E-04 | 0.118311E+00 | 0.435337E-03 |
| 20.5 | 0.175710E-01 | 0.915704E-01 | 0.832900E-04 | 0.105326E+00 | 0.164616E-03 |
| 21.0 | 0.161445E-01 | 0.840575E-01 | 0.779125E-04 | 0.972269E-01 | 0.133763E-03 |
| 21.5 | 0.157725E-01 | 0.754137E-01 | 0.760743E-04 | 0.765733E-01 | 0.387992E-03 |
| 22.0 | 0.147779E-01 | 0.710599E-01 | 0.701914E-04 | 0.695287E-01 | 0.460478E-03 |
| 22.5 | 0.133834E-01 | 0.616862E-01 | 0.719602E-04 | 0.721770E-01 | 0.175355E-03 |
| 23.0 | 0.113846E-01 | 0.537475E-01 | 0.677819E-04 | 0.778912E-01 | 0.135866E-03 |
| 23.5 | 0.876339E-02 | 0.434412E-01 | 0.647312E-04 | 0.109545E+00 | 0.129361E-03 |
| 24.0 | 0.808895E-02 | 0.346752E-01 | 0.642453E-04 | 0.681020E-01 | 0.153908E-03 |
| 24.5 | 0.777060E-02 | 0.300342E-01 | 0.583207E-04 | 0.150422E-01 | 0.118910E-03 |
| 25.0 | 0.656817E-02 | 0.302435E-01 | 0.560719E-04 | 0.932754E-01 | 0.148538E-03 |

**Table S11.** Parameters of one-component Debye's model for compound **4**.

| $T$ / K | $\chi_S$ / (cm$^3$ mol$^{-1}$) | $\chi_T$ / (cm$^3$ mol$^{-1}$) | $\tau$ / (s) | $\alpha$ | ***Residual*** |
|---|---|---|---|---|---|
| 2.0 | 0.745569E+00 | 0.178618E+01 | 0.198896E-03 | 0.647895E-01 | 0.216016E-02 |
| 2.3 | 0.655226E+00 | 0.169201E+01 | 0.190313E-03 | 0.496632E-01 | 0.140887E-02 |
| 2.6 | 0.584512E+00 | 0.159311E+01 | 0.174700E-03 | 0.387469E-01 | 0.752514E-03 |
| 2.9 | 0.527696E+00 | 0.148984E+01 | 0.155002E-03 | 0.298183E-01 | 0.560686E-03 |
| 3.2 | 0.480440E+00 | 0.138971E+01 | 0.134592E-03 | 0.237241E-01 | 0.518183E-03 |
| 3.5 | 0.441056E+00 | 0.129592E+01 | 0.115412E-03 | 0.186770E-01 | 0.495843E-03 |
| 3.8 | 0.407432E+00 | 0.121095E+01 | 0.982747E-04 | 0.157286E-01 | 0.406689E-03 |
| 4.1 | 0.379333E+00 | 0.113244E+01 | 0.835653E-04 | 0.119770E-01 | 0.424789E-03 |
| 4.4 | 0.354964E+00 | 0.105994E+01 | 0.709397E-04 | 0.734079E-02 | 0.549561E-03 |
| 4.7 | 0.333692E+00 | 0.997073E+00 | 0.607261E-04 | 0.519379E-02 | 0.425995E-03 |
| 5.0 | 0.314959E+00 | 0.939640E+00 | 0.522004E-04 | 0.296761E-02 | 0.567185E-03 |

**References：**


1. O. V. Dolomanov, L. J. Bourhis, R. J. Gildea, J. A. K. Howard and H. Puschmann, OLEX2: a complete structure solution, refinement and analysis program, J. Appl. Crystallogr., 2009, **42**, 339-341
2. G. Sheldrick, SHELXT - Integrated space-group and crystal-structure determination, *Acta Crystallographica Section A*, 2015, **71**, 3-8.
3. G. Sheldrick, Crystal structure refinement with SHELXL, *Acta Crystallographica Section C*, 2015, **71**, 3-8.
4. A. Schäfer, H. W. Horn and R. Ahlrichs, Fully optimized contracted Gaussian basis sets for atoms Li to Kr, *J. Chem. Phys.*, 1992, **97**, 2571-2577.
5. W. R. Wadt and P. J. Hay, Ab initio effective core potentials for molecular calculations. Potentials for main group elements Na to Bi, *J. Chem. Phys.*, 1985, **82**, 284-298.
6. G. Scalmani and M. J. Frisch, Continuous surface charge polarizable continuum models of solvation. I. General formalism, *The Journal of chemical physics*, 2010, **132 11**, 114110.
7. R. Bauernschmitt and R. Ahlrichs, Treatment of electronic excitations within the adiabatic approximation of time dependent density functional theory, *Chem. Phys. Lett.*, 1996, **256**, 454-464.
8. Scalmani G, Frisch MJ, Mennucci B, Tomasi J, Cammi R, Barone V. Geometries and properties of excited states in the gas phase and in solution: theory and application of a time-dependent density functional theory polarizable continuum model. *J. Chem. Phys*. 2006, **124**, 094107.